Critical Heat Flux Enhancement Mechanism by Surface Modification based on Hydrodynamic Instability Model

Han Seo and In Cheol Bang*
School of Mechanical and Nuclear Engineering
Ulsan National Institute of Science and Technology (UNIST)
50 UNIST-gil, Ulju-gun, Ulsan, 689-798, Republic of Korea
icbang@unist.ac.kr

ABSTRACT

This paper presents surface modifications based on hydrodynamic instability model to enhance critical heat flux (CHF). Experimental observations of the CHF performance based on the surface modifications were performed in a plate pool boiling facility using an FC-72 refrigerant under saturation conditions. Temperature distribution and CHF condition of each heater surface were determined using an infrared thermometry. Four types of heater surfaces were considered: plain, 9 and 64 pillars, and 9 holes. The CHF performance of the plain and 9 and 64 pillars heating surfaces showed similar trend (148 kW/m^2). For the 9 holes heating surface, the CHF performance was increased by 20%, compared to other heating surfaces (174 kW/m^2). Rayleigh–Taylor (RT) instability observation at the CHF condition for the plain and 9 holes heating surfaces were conducted to show the relation between the RT instability wavelength and the CHF condition. The hot spots for the 9 holes heating surface were isolated in the patterned surfaces before the CHF was reached, while the hot spots of the other surfaces were coalesced at high heat fluxes. The hydrodynamic theory by changing the RT instability wavelength based on the surface modification can explain the CHF enhancement mechanism.

KEYWORDS
Critical heat flux, Hydrodynamic theory, Rayleigh–Taylor wavelength, Helmholtz wavelength

1. INTRODUCTION

Analysis of boiling heat transfer has been widely conducted because an efficient heat transfer would be achieved during nucleate boiling. A latent heat, which is the phase change heat transfer energy from liquid to vapor, is delivered in the nucleate boiling region. However, there is a critical heat flux (CHF) point, which is the upper limit for efficient heat removal in the nucleate boiling. Power industries determine the operational upper bound related to the CHF. If the power density of a device exceeds the CHF point, bubbles and vapor films will be covered on the whole heater surface. Because vapor films have much lower heat transfer capabilities compared to the liquid layer, the temperature of the heater surface will increase rapidly, and the device could be damaged due to the heater burnout. Therefore, the prediction and the enhancement of the CHF are essential to maximizing the efficient heat removal region.
Numerous studies have been conducted to describe the CHF phenomenon, such as hydrodynamic instability theory, macrolayer dryout theory, hot/dry spot theory, and bubble interaction theory. The hydrodynamic instability model, proposed by Zuber [1], is the predominant CHF model that Helmholtz instability attributed to the CHF. Zuber [1] assumed that the critical Taylor wavelength is related to the

* Corresponding author : Tel.:+82-52-217-2915, Fax:+82-52-217-3008
E-mail: icbang@unist.ac.kr (In Cheol Bang)

Helmholtz wavelength. Lienhard and Dhir [2] proposed a CHF model that Helmholtz wavelength is equal to the most dangerous Taylor wavelength. In addition, they showed the heater size effect using various heater surfaces. Lu et al. [3] proposed a modified hydrodynamic theory that the Helmholtz instability was assumed to be the heater size and the area of the vapor column was used as a fitting factor. The modified hydrodynamic theories were based on the change of Helmholtz wavelength related to the Taylor wavelength.

In the present study, the change of the Rayleigh–Taylor (RT) instability wavelength, based on the heater surface modification, was conducted to show the CHF enhancement based on the hydrodynamic theory in a plate pool boiling. Sapphire substrate was used as a heater substrate, and the heater surface modifications were performed on the Pt surface to show the change of the CHF.

2. EXPERIMENTAL SETUP

The experiment using Pt surfaces was conducted in a pool boiling facility. In a boiling channel, there are four cartridge heaters and a condenser to maintain the saturation state of the working fluid during the experiment. A gold-coated reflection mirror is located at the bottom of the inner vessel to pass the IR intensity to the IR thermometry. An SC7210 IR thermometry (FLIR systems) is used for characterizing the heater surface. The calibration of the IR intensity to convert heater surface temperature from IR intensity is done via a thermocouple attached on the heater surface. The calibration progress is conducted for every heater surface. Using calibration process, the maximum error is less than 1%, 0.5 °C.
A sapphire substrate with 1 mm thickness was used as the substrate material because it has high optical and high thermal transmissions. On the sapphire substrate, plain and patterned Pt surfaces were prepared to show the effect of heater geometry. The Pt material is opaque at the IR range (3–5 μm), thus measuring the temperature profile of the Pt surface is possible. The Pt layer was deposited on the sapphire substrate with the area of 50 mm × 20 mm. K575X (Quorum Technologies) sputter coater was used as the Pt deposition device. The Au electrodes are printed at the end of the Pt surface with dimensions of 15 mm × 20 mm. Finally, the heating area of the Pt surface is 20 mm × 20 mm. After deposition of the Au electrode, annealing (200°C, 1hr) was conducted. The resistance of the Pt layer was read by the standard resistance. A data acquisition system (DAS) was used to read the voltage and the current of the heating surface.

As heating surfaces, four kinds of heating surfaces were prepared: plain, 9 pillars, 64 pillars, and 9 holes. Figure 1 shows the images of the heater surfaces, which were used in the experiment. For the pillars heating surfaces, two kinds of patterned surfaces were prepared: 3 mm × 3 mm with 6 mm pitch and 1.5 mm × 1.5 mm with 3 mm pitch. For the Pt holes heating surface, 3 mm × 3 mm with 6 mm pitch was prepared on the plain Pt surface. The patterned surface has the shape of square.

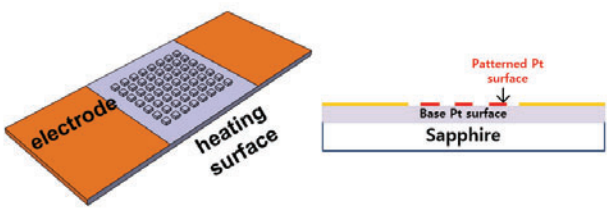

(a)

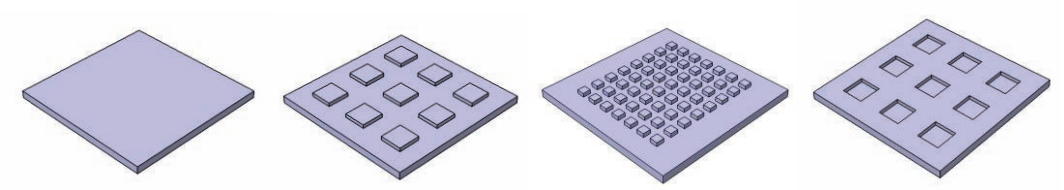

(b) (c) (d) (e)

Figure. 1. Patterned Pt surfaces: (a) heating geometry, (b) plain, (c) 9 pillars, (d) 64 pillars, (e) 9 holes.

With the Pt heating surfaces, pool boiling experiments were conducted using FC-72 refrigerant. This working fluid is highly wettable with any surface because it has low surface tension (0.01 N/m) compared to water. During the experiment, the heat flux was increased stepwise until the CHF was occurred. When there was a sufficient margin for the CHF, the heat flux was increased to ~10 kW/m^2 until a steady state was observed. The input of the heat flux was then set to ~1 kW/m^2 as the CHF was approached.

Figure 2(a) shows the SEM images of the patterned Pt surfaces and the Fig. 2 (b) indicates the actual heating surfaces; plain, 9 and 64 pillars, and 9 holes. As shown in Fig. 2(a), the Pt surface was confirmed to be non-porous. The thickness of the Pt surface was calculated by 30 nm, based on the deposition time and current of the sputtering device.

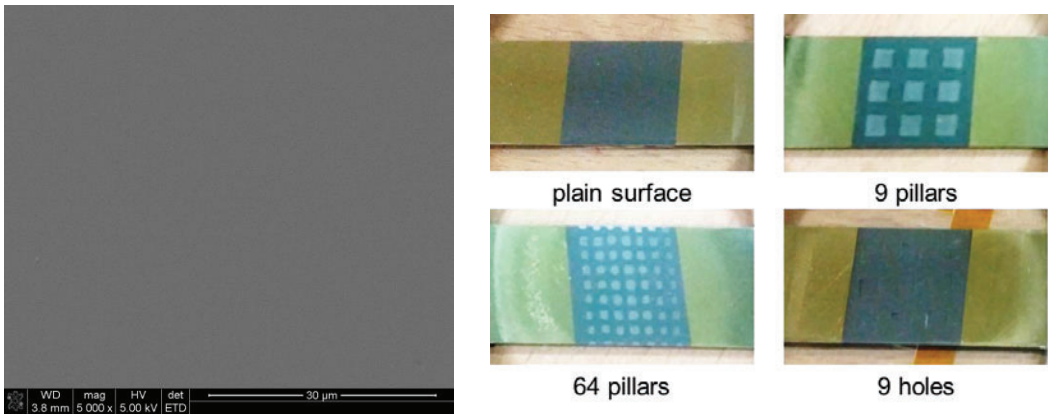

(a) (b)

Figure 2. Pt heating surfaces: (a) SEM observation of the Pt surface, (b) actual heating surfaces

3. RESULTS AND DISCUSSION

In the experiment, CHF phenomenon was always generated with a sudden increase in the heater surface temperature. After the CHF is reached, the film boiling state can be observed if the heat flux is controlled; however the heater can burnout if the heat flux is not controlled. In the present work, the average CHF value of the plain Pt surface was obtained as 148 kW/m^2. The obtained CHF value of the plain surface had the same value that of the Zuber's CHF value [1]. For 9 pillars and 64 pillars, the values of CHF were 149 and 147 kW/m^2, respectively. For 9 holes heating surface, however, the CHF was increased by 174 kW/m^2, 20% enhanced CHF was observed.

Figure 3 shows the boiling curves for the plain, 9 and 64 pillars, and 9 holes heater surfaces. The experiment was conducted three times for each heater type and the boiling curves indicated the average experimental results. As shown in Fig. 3, boiling heat transfer between the plain and 9 holes heating surfaces showed similar performance, but the boiling heat transfer of the 9 and 64 pillars heating surfaces was degraded.

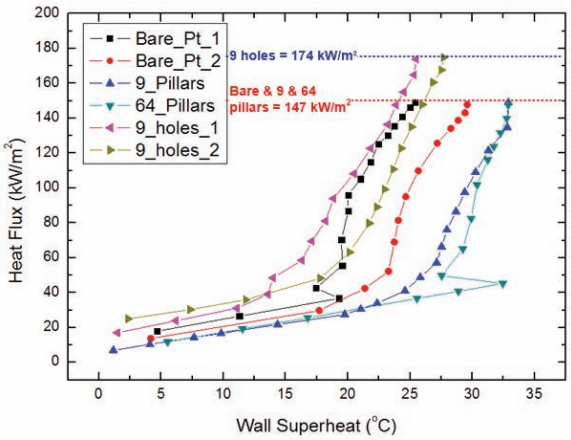

Figure 3. Boiling curve for each heater surface

Figure 4 shows temperature distributions of heating surfaces at various heat fluxes (50, 100, 140, and 170 kW/m^2). The same temperature legend was used for comparison. As Fig. 4 shows, the maximum temperature and average temperature of the 9 holes at each heat flux were lower than those of the other heaters. Distinguished temperature distribution was observed in the 9 and 64 pillars and 9 holes heater surfaces. The hot and cold spots were observed in the patterned surfaces even though the thickness different between the plain surface and patterned surface was 30 nm. In the 9 and 64 pillars, the cold spots were observed in the pillar surfaces. In the 9 holes, the hot spots were observed in the patterned hole. This means that hot spots of the 9 holes heating surface would not be coalesced until the critical point is reached. On the other hand, hot spots of the 9 and 64 pillars heating surfaces were distributed whole heating surfaces except for the patterned area. By isolating hot spots in the 9 holes heating surface, the enhanced CHF was observed. The maximum averaged heat transfer coefficients at a certain heat flux were 5.86 kW/m^{2}K for the of the plain heating surface, whereas those for the 9 and 64 pillars heating surfaces were 4.53 and 4.48 kW/m^2, respectively. On the other hand, the 9 holes heating surface was calculated as 4.82 kW/m^{2}K.

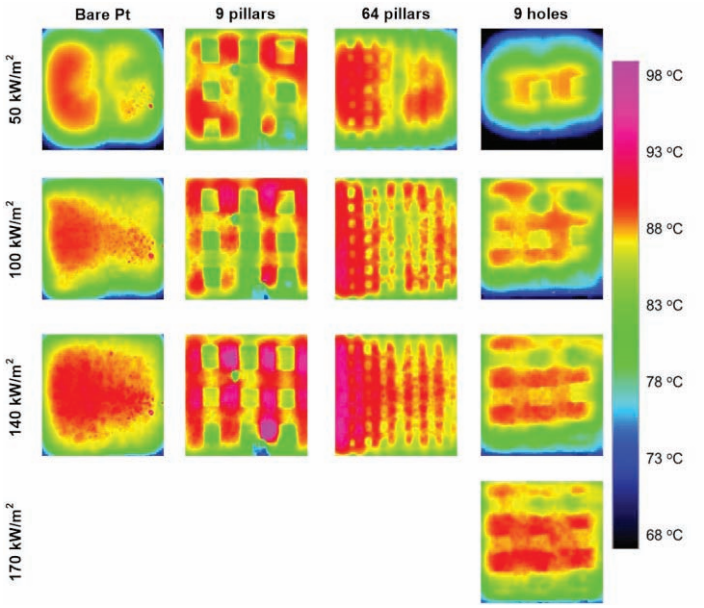

Figure 4. Temperature fields of plain, 9 pillars, 64 pillars, and 9 holes heating surfaces at various heat fluxes.

Many theories have been suggested to describe the CHF phenomenon based on the hydrodynamic instability, macrolayer dryout, hot/dry spots, and bubble interaction theory. The CHF is recognized as the maximum latent energy transport from the heating surfaces; thus, the hydrodynamic equation can be expressed as

$$q''_{CHF} \equiv u_c h_{fg} \rho_g \frac{A_g}{A_h} \quad (1)$$

$$u_c = \sqrt{\frac{2\pi\sigma}{\rho_g \lambda_H}} \quad (2)$$

where u_c is the critical vapor velocity, h_{fg} is the latent heat of the working fluid, ρ_g is the vapor density, and A_g and A_h are the area of the vapor column and heater surface, respectively. The critical vapor velocity is a form of the Helmholtz instability wavelength. Zuber assumed that the Helmholtz instability wavelength is a form of the RT instability wavelength [1]. Therefore, Zuber proposed the hydrodynamic instability CHF model based on the critical vapor velocity:

$$q''_{CHF} = \frac{\pi}{24} \rho_g^{1/2} h_{fg} \sqrt[4]{g\sigma(\rho_f - \rho_g)} \quad (3)$$

where ρ_f and ρ_g are the liquid and vapor densities, respectively, h_{fg} is the latent heat of the working fluid, and σ is the surface tension of the working fluid. In Zuber's theory, the Helmholtz instability wavelength was assumed to be a relation of the RT instability wavelength. The RT instability wavelength can be defined as:

$$\lambda_{Tc} = 2\pi \left[\frac{\sigma}{g\left(\rho_f - \rho_g\right)} \right]^{1/2} \quad (4)$$

$$\lambda_{Td} = 2\sqrt{3}\pi \left[\frac{\sigma}{g\left(\rho_f - \rho_g\right)} \right]^{1/2} \quad (5)$$

The critical and the most dangerous wavelength of the FC-72 are 4.9 and 8.5 mm, respectively. In the present study, we assumed that Helmholtz instability wavelength is equal to the most dangerous wavelength. If the patterned surface changed the RT instability wavelength based on the heater geometry, the RT instability wavelength of the 9 holes heating surface would be changed from 8.5 mm to 6 mm. The modified wavelength brings the change of CHF based on the hydrodynamic theory:

$$n = \left(\lambda_{Td} / \lambda_{\mathrm{mod}} \right)^{0.5} \quad (6)$$

where n is the change of CHF ratio. The modified RT instability wavelength brings 19% CHF enhancement compared to the plain surface (most dangerous wavelength), which has the similar enhancement value obtained from the experiment. Therefore, the patterning surface, especially for the 9 holes heating surfaces, could change the bubble columns (RT instability wavelength) and bring the CHF enhancement by changing the critical vapor velocity.

The modified RT wavelength would be obtained at the CHF region. The theories of modified hydrodynamic limits do not provide any experimental proof for the changing RT instability wavelength

[5-7]. Therefore, an experiment on measuring the change in the RT instability wavelength for the heating surfaces is needed to show the relation of the RT instability wavelength with the CHF. The RT instability wavelength at the CHF can be recognized as the region where the vapor film on the heater surface fully develops. Therefore, the most dangerous wavelength could be formed at the CHF region. The RT instability wavelength observation for the plain and the 9 pillars was conducted to find the relation between the CHF and the RT instability wavelength. Fig. 5 shows the RT instability observation at the CHF point. As shown in Fig. 5(a), the number of vapor column of the plain surface was 3 at horizontal direction. The pitch of the wavelength is less than 10 mm. The obtained RT instability wavelength showed a similar with the calculated λ_{Td}. On the other hand, the RT instability of the 9 holes heating surface showed a short length of the RT wavelength compared to the plain surface. However, the change of the wavelength was small to measure the difference between the plain and 9 holes heating surfaces. Based on the RT instability observation at CHF region, the modified RT instability based on heater modifications could bring CHF enhancement.

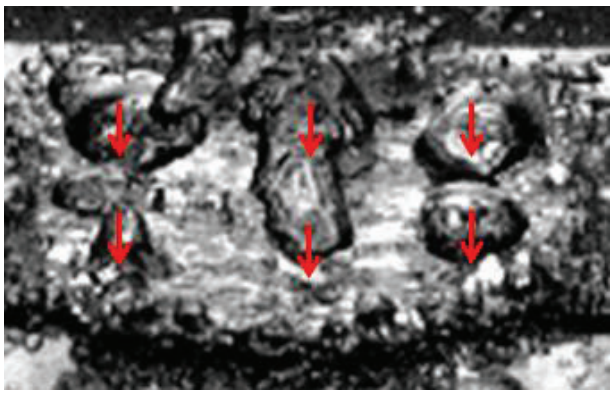

(a)

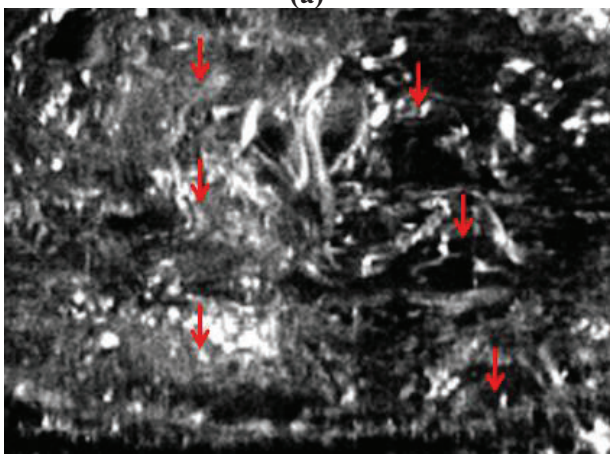

(b)

Figure 5. RT instability wavelength: (a) plain, (b) 9 holes heating surfaces.

4. CONCLUSIONS

In the present work the study of the CHF was conducted using plain and patterned heating surfaces. The following conclusions are obtained.

(1) The average CHF value of the plain heating surface was obtained as 148 kW/m^2. For 9 and 64 pillars heating surfaces, the CHF values were 149 and 147 kW/m^2, respectively. On the other hand, the CHF value of 9 holes heating surfaces showed 20% CHF enhancement (174 kW/m^2) was obtained.

(2) The hot spots of the 9 holes heating surface were isolated at the patterned surface, while the hot spots of the 9 and 64 pillars heating surfaces were gathered except for the patterned area. The isolation of the hot spots would delay the CHF.
(3) Modified RT instability wavelength based on the heater modification could explain the CHF enhancement.

ACKNOWLEDGMENTS

This work was supported by the Nuclear Energy Research Program through the National Research Foundation of Korea (NRF) funded by the Ministry of Science, ICT, and Future Planning (2013M2B2B1075734, 2013M2A8A1041442).

REFERENCES

1. N. Zuber, "Hydrodynamic Aspects of Boiling Heat Transfer," Ph.D Thesis, Univ. of California (1959).
2. J. H. Lienhard and V. K. Dhir, "Extend Hydrodynamic Theory of the Peak and Minimum Pool Boiling Heat Fluxes," NASA CR-2270, Contract No. NGL 18-001-035 (1973).
3. M. Lu, R. Chen, V. Srinivasan, V. P. Carey,, A. Majumdar, "Critical heat flux of pool boiling on Si nanowire array-coated surfaces," *International Journal of Heat and Mass Transfer*, **54**, pp. 5359-5367 (2011).
4. M. Lu, C. Huang, C. Huang, Y. Chen, "A modified hydrodynamic model for pool boiling CHF considering the effects of heater size and nucleation site density," *International Journal of Thermal Science*, **91**, pp. 133-141 (2015).
5. C. S. Liter, M. Kaviany, "Pool-boiling CHF Enhancement by Modulated Porous-layer Coating: Theory and Experiment," *International Journal of Heat and Mass Transfer*, **44**, pp. 4287-4311 (2001).
6. S. D. Park, S. W. Lee, S. Kang, I. C. Bang, J. H. Kim, H. S. Shin, D. W. Lee, D. W. Lee, "Effects of Nanofluids Containing Graphene/Graphene-oxide Nanosheets on Critical Heat Flux," *Applied Physics Letters*, **97**, 023103 (2010).
7. S. W. Lee, S. D. Park, I. C. Bang, "Critical heat flux for CuO nanofluid fabricated by pulsed laser ablation differentiating deposition characteristics," *International Journal of Heat and Mass Transfer*, **55**, pp. 6908-6915 (2012).